CHAOTIC WATER DROP EXPERIMENT

1. Introduction

Dripping water from a faucet is a well-known example of chaotic dynamical systems easily seen in daily life. O.E. Rössler introduced the dynamics of a leaky faucet as a model of a nonlinear chaotic system in 1977. He suggested that the formation of water drops at the nipple of a faucet could exhibit chaotic behavior. This was confirmed initially by R. Shaw and later by Martien, et al. In 1985, Martien, et al. launched thorough investigation of behaviors at various flow rates and collection of chaotic attractors for the system. Period doubling was widely studied in leaky faucet dynamics. Other interesting phenomena were seen, such as tangent intermittence, quasi-periodicity and boundary crisis, and Hopf bifurcation. Since the original pioneering with the study of the leaky faucet, many experimental and theoretical improvements upon the apparatus and the mathematical model have been made by many researchers over the years.

The use of modern technology has allowed for extensive study of the formation of the droplets of water. Buch et al. used a high-speed digital video camera to allow a better understanding of the dynamics of the system by showing details of drop oscillations, formation, and separation of the droplets. With this information, some parameters of the system are better understood. Kiyono and Fuchikami have developed equations that consider the fluid dynamics of the droplets more thoroughly.

In this experiment, you will study the path to chaos as a function of flow rate, and try to identify strange attractors with a standard leaky faucet apparatus. This is an open-ended experiment and you are encouraged to explore the dynamics of leaky faucet as your time permits. You may need to refer to references to widen your understanding of the underlying theoretical and experimental aspects.

2. Theory

For a theoretical analysis of the complex phenomena observed in the dripping faucet, a simple model treating the formation and the falling of the drop as a damped harmonic oscillator with a variable mass is generally adopted:

$$\frac{d}{dt}\left(m\frac{dx}{dt}\right) = -kx - b\frac{dx}{dt} + mg \qquad (1)$$

$$\frac{dm}{dt} = R \qquad (2)$$

where x is the position of the center of mass of the forming drop, m is its mass, g is the gravitational acceleration, k is the spring constant, b is the damping parameter, t is the time, and R is the flow rate (mass per unit time) . Here k represents the surface tension of the liquid and b depends on the liquid viscosity and on the nozzle characteristics. When the downward displacement of the water reaches a critical value x_c, the mass is suddenly reduced by ΔM and the position of the remaining mass oscillates according to (1) and changes according to (2).

The behavior of the model depends critically on the mechanism used to simulate the release of a drop. Both the mass of the falling drop and the initial conditions for the residual mass should be determined. Theoretically, the drop mass ΔM can be produced in several ways, and three popular mechanisms are:

$$\Delta M = \alpha M_c \qquad (3.1)$$

$$\Delta M = \alpha v_c \qquad (3.2)$$

$$\Delta M = \alpha M v_c \qquad (3.3)$$

The best choice seems to be the last one, Eq. 3.3 since the mechanism of the release of the drop with a mass proportional to momentum seems to be more realistic and in better agreement with experimental results. In addition to the determination of the mass of each falling drop, the initial conditions for the residual mass must be specified. Regarding the breaking of the drop at the critical point x_c, two different models have been proposed:

(a) A spherical drop and a residue point mass,

(b) Two spherical drops, one falling off, the other forming a residue for the next drop.

In the first model, given the system center of mass to be at x_c, the initial position for the residue mass is given by:

$$x_0 = x_c - r\frac{\Delta M}{M_c} \quad . \tag{4}$$

where $r = \left(\frac{3\Delta M}{4\pi\rho}\right)^{\frac{1}{3}}$ and ρ is the liquid density (Fig. 1a). Whereas in the second model the position of the residue is given by:

$$x_0 = x_c - \left(r_1 + r_2\right)\frac{\Delta M}{M_c} \tag{5}$$

where $r_{1,2} = \left(\frac{3\Delta M_{1,2}}{4\pi\rho}\right)^{\frac{1}{3}}$ and $M_1 = \Delta M$, $M_2 = M_c - \Delta M$ (Fig.1b). In both models, the initial velocity of the residue is set equal to v_c.

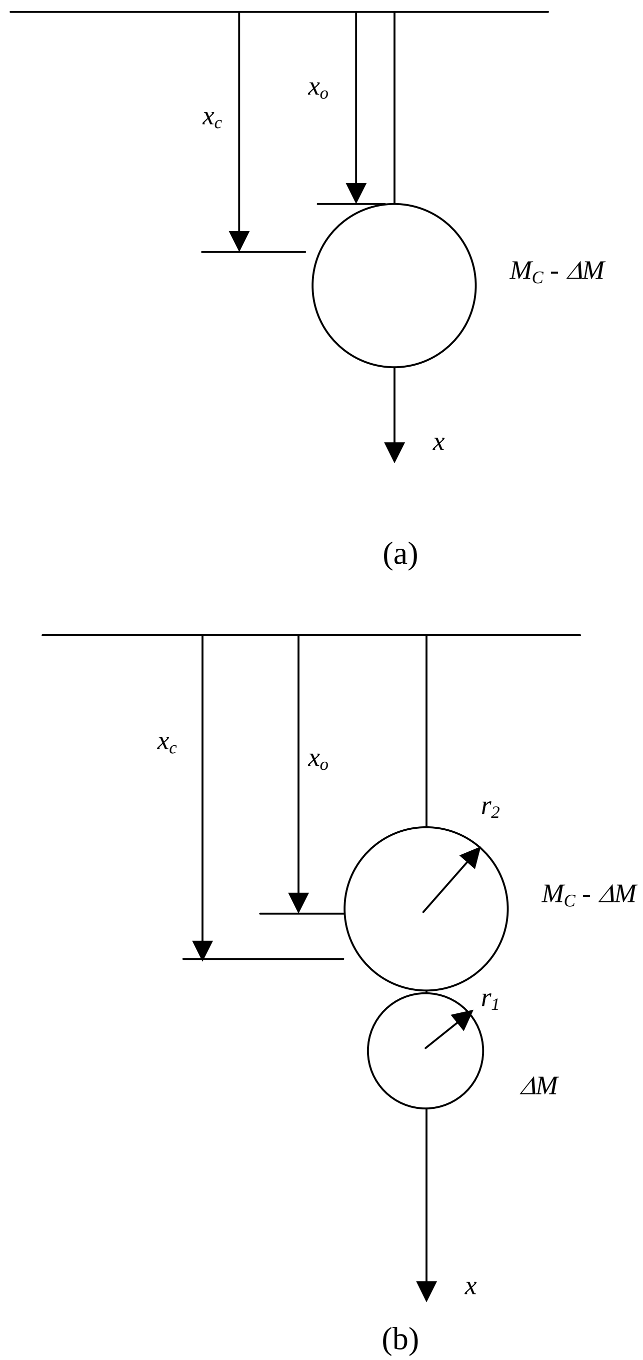

Figure 1. Mechanism of drop breaking at the threshold: (a) one-sphere and (b) two-sphere models

Exact solutions of equations (1) and (2) is not easily realized. One could assume an approximate equation of a damped-oscillation form:

$$x(t) = At^{\frac{1}{3}} + B\sin(\omega t^{\frac{2}{3}} + \Omega_i)e^{-\gamma t} \qquad (6)$$

This would explain the repeats of period-one and period-two motion in a bifurcation diagram in terms of a feed back loop in the phase angle Ω_i .

One could successfully reproduce bifurcation diagrams including the period-doubling transition to chaos from both the approximate equation (6) and from the numerical integration of equations (1) and (2).

Applying fluid dynamical computations and one can find that the breakup of a drop occurs through two main processes. The first part is obviously the break off of the main drop. The second part, immediately after the separation of the main drop, is the necking in the fluid left on the tip of the faucet in which surface tension is a restoring force, ultimately causing the formation of a secondary, or satellite, droplet. We should treat the spring constant *k* as a function of mass, to allow the mass-spring model to be more realistic. Then the equation of motion is as follows:

$$m\frac{d^2z}{dt^2} + \left(\frac{dz}{dt} - v_0\right)\frac{dm}{dt} = -kz - \gamma\frac{dz}{dt} + mg \qquad (7)$$

where the position *z* of the mass point in this model corresponds to the position z_G of the center of gravity of the drop of fluid (approximated to an integral number of cylindrical disks acting under gravity). The second term in the equation represents adhering of mass with a relative velocity. The mass increases as in (2), with $R = \pi a^2 v_0$, *a* being the radius of the faucet nozzle. The mass-dependent spring constant varies linearly with mass and the equation is initially determined by *a* and the boundary condition that the spring constant equals zero when the mass undergoes free-fall. This method is unique in the consideration that it implies that the dripping time interval is decided uniquely from the value of the previous mass left on the nozzle after the break off of the falling drop. Their model allowed for the natural occurrence of necking after drop formation and showed that it had and integral role in determining the dripping time interval. Although the model is based on a one-dimensional map system, it will reproduce a variety of dynamical behaviors seen in many experiments systematically.

3. Experimental Set-Up

The schematic design of the experimental apparatus is presented in Figures 2 and 3. The apparatus consists of an insulated plastic jug with a reservoir jug atop a stool connected to its top. Water is siphoned from the reservoir jug to the insulated jug, ensuring a consistent water level and therefore a consistent pressure associated with the flow rates. Without the extra reservoir of water, the water level inside the insulated jug would not be maintained and the flow rate of the water would decrease linearly with the decreasing height of the water. It must be noted, however, that all sets of data were collected over a small period of time. The assumption can then be made that the water level stayed fairly constant and flow rate was not affected, allowing some error in the ability of the siphon to keep a constant level of water. Drift, or the drifting of the apparatus from one constant flow rate to another without any external interference, is inevitable. Taking data sets over relatively short periods of time also minimizes this effect.

A narrow glass tube with a flow rate control valve extends from the bottom of the jug down an I-beam, to which the whole apparatus is rigidly attached. At the end of the beam, the glass tube bends down and ends. Two stacked funnels surround the end of the glass tube and protect it from ambient air drafts and other phenomena that might disrupt the drop rate or the alignment of the drops with the sensory mechanism. The funnels also assist in deterring the occurrence of "double pulsing". When the laser light passes through the very center of the water drop, the geometry allows for light to be detected by the sensory mechanism, causing one water drop to look like two small ones. The translucent funnels diffuse the laser beam so that at no point does the beam fully traverse the middle of the water drop, yielding accurate data. However, to make sure there is not a problem of double pulsing, practically one can tinker a bit with the position of the funnel.

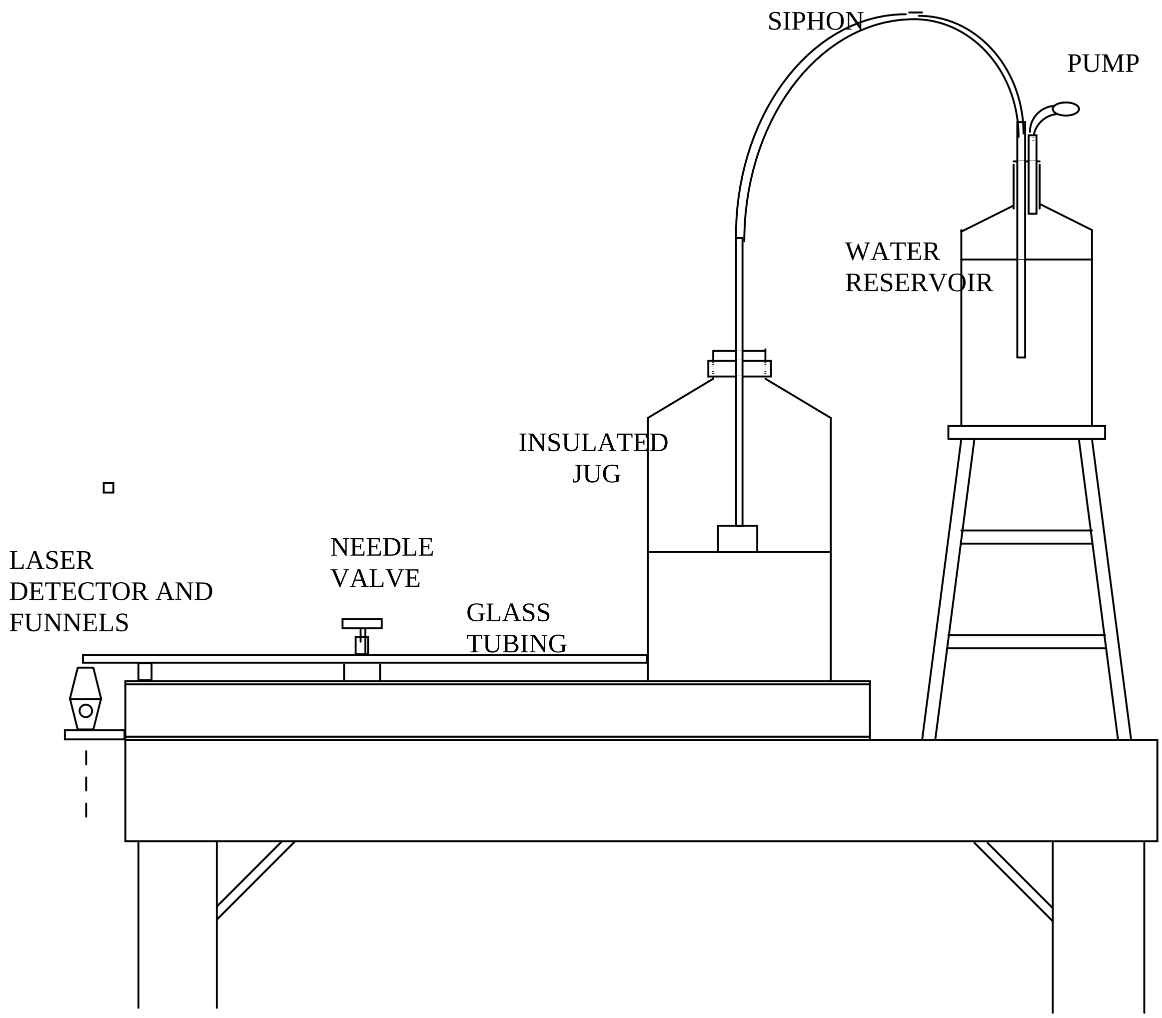

Figure 2. Experimental set-up for the chaotic faucet.

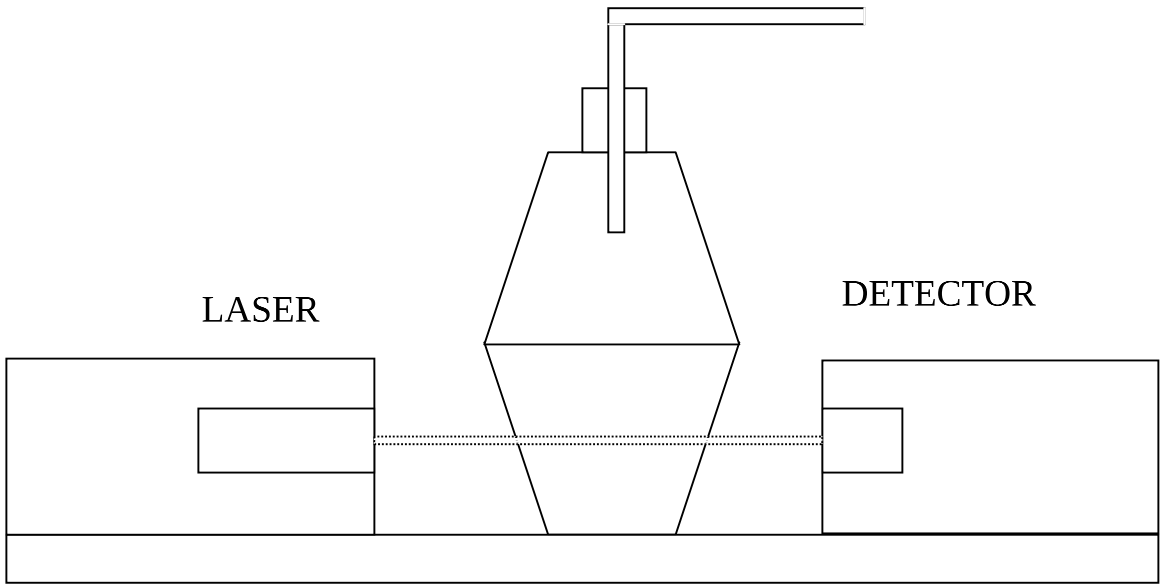

Figure 3. Laser detection system used to detect water drops.

The sensory mechanism is a very simple optical electronic device (laser + phototransistor detector), which measures the drop width and the time interval between them. When a water drop intercepts the laser beam, the phototransistor detector circuit emits a pulse. The pulse is sent to the DAQ circuitry. The DAQ circuit transforms the analog pulse from the water drop to a square pulse, and then measures the width of the pulse and the elapsed time interval since the last drop. From there, the information is sent to a computer running a LabWindows CVI analysis program with the capability to store the data and create various plots.

The LabWindows/CVI computer program, called "H2O_Drop2.c" is a typical data acquisition program that is for all intents and purposes self-explanatory. Before running this program for the first time, press "Init DAQ" to initialize the DAQ system. This only needs to be done once at the very beginning, after loading the program. To start data collection, press "Start," and to stop data collection, press "Stop." Only after data collection is stopped can various on-line plots be selected from the pull-down menus and printed, one of which is shown in the figure below. One small detail that must be attended to during data collection is the correlation of the clock driving the DAQ circuit (selected on the top of the circuit) and the computer program (selected from the left most pull-down menu). By switching between 10 kHz and 100 kHz clocks one can overcome the problem of counter overflow. Since the circuit uses digital counters with a finite maximum count to determine the time between pulses if a drop happens to be unnaturally wide or similarly the time between drops excessively long (the limits being 0.32768 s for 100 kHz and 3.2768 s for 10 kHz signal) the counters will roll over from their maximum values back to zero, which may cause an error in time interval readings.

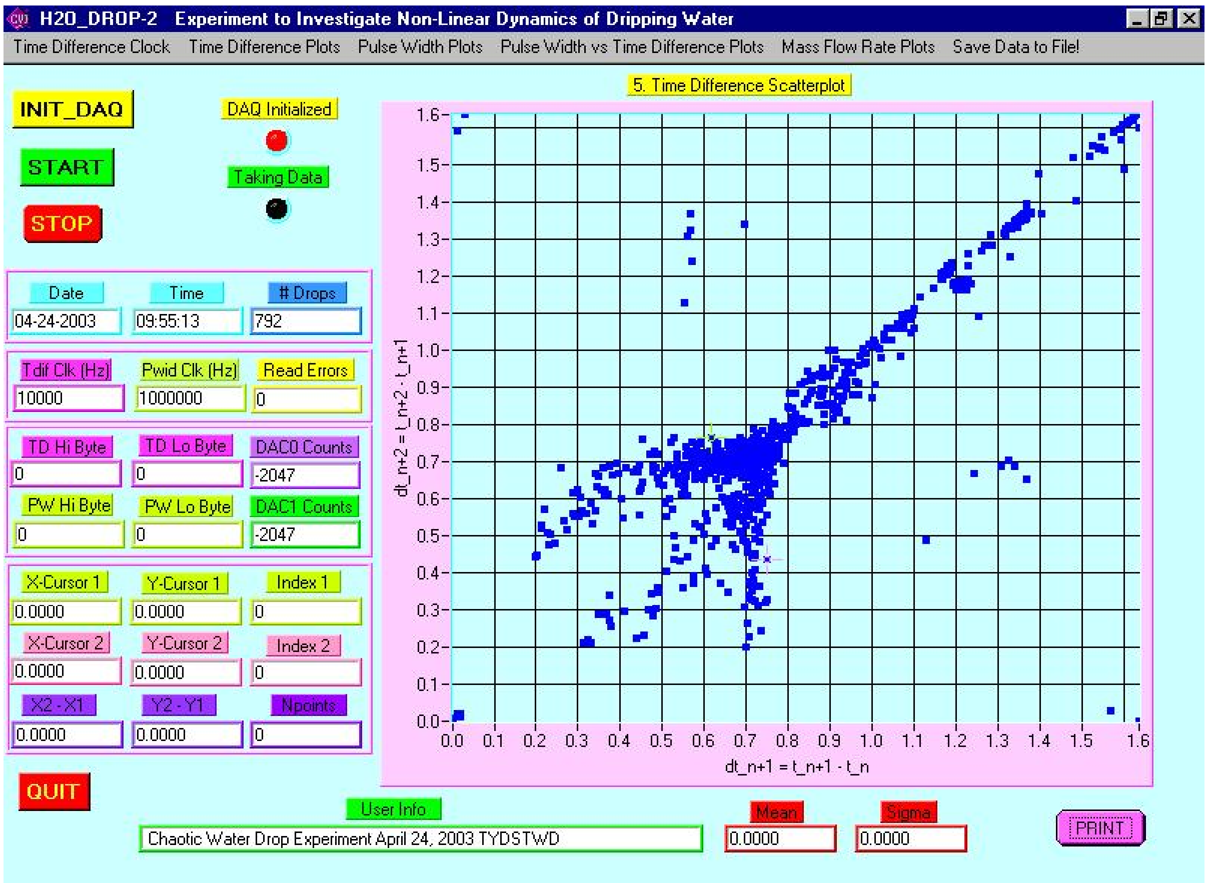

Figure 4. H2O_Drop-2 on-line plot of $\Delta t_{n+2} \equiv (t_{n+2} - t_{n+1})$ vs. $\Delta t_{n+1} \equiv (t_{n+1} - t_n)$.

4. Data Analysis

The most useful way of representing data obtained from the chaotic faucet is drawing a return map. Return maps are generally used in analyzing chaotic systems. In a return map drawn by the computer program you focus on three drops at a time; the time between the first and the second is taken to be the x-coordinate of the return map, the time between the second and the third is taken to be the y-coordinate. When this process is continued for drops one to three, than two to four, and so on, a scatter plot of points t_n vs. t_{n+1} is obtained. The computer program also produces a similar graph of relative drop widths. When the time interval between drops or the drop widths are constant, the return map will consist of one point. But when they change in time, the return map will show various structures according to the behavior of the system.

In this experiment, the aim is to investigate the dynamical behavior of the dripping faucet by creating time interval and pulse width return maps. Begin the experiment from low flow rates. As you increase the flow rate, you will observe the transitions from periodic behavior to chaotic behavior. Determine the critical drop rates where bifurcations and chaotic attractors are found. Which flow rates would guarantee period-1 (or a single period) motion? Discuss other quasi-periodic motions and attractors that you observed.

5. References

[1] O.E. Rössler, Synergetics, A workshop, H. Haken (Ed.), Springer Berlin, 1977, p. 174.

[2] R. Shaw, The dripping faucet as a model chaotic system, Aerial Press, Santa Cruz, USA, 1984.

[3] P. Martien, S.C. Pope, P.L. Scott, R.S. Shaw, Phys. Lett. A 110 (1985) 399.

[4] H.N. Núñez-Yépez, A.L. Salas-Brito, C.A. Vargas, L. Vincente, Eur. J. Phys. 10 (1989) 99.

[5] X. Wu, Z.A. Schelly, Physica D 40 (1989) 433).

[6] R.F. Cahalan, H. Leidecker, G.D. Cahalan, Comp. Phys. 3 (1990) 368.

[7] K. Dreyer, F.R. Hickey, Am. J. Phys. 59 (1991) 619.

[8] J. Austin, Phys. Lett. A 155 (1991) 148.

[9] J.C. Sartorelli, W.M. Goncalves, R.D. Pinto, Phys. Rev. E 5 (1994) 3963.

[10] R.D. Pinto, W.M. Goncalves, J.C. Sartorelli, M.J. de Oliveira, Phys. Rev. E 52 (1995) 6896.

[11] T.J.P. Penna, P.M.C. de Oliveira, J.C. Sartorelli, W.M. Goncalves, R.D. Pinto, Phys. Rev. E 52 (1995) R2168.

[12] Z. Néda, B. Bako, E. Rees, Chaos 6 (1996) 59.

[13] J.G.M. da Silva, J.C. Sartorelli, W.M. Goncalves, R.D. Pinto, Phys. Lett. A 226 (1997) 269.

[14] A. D'Innocenzo, L. Renna, Phys. Rev. E 58 (1998) 6847.

[15] A. Tufaile, R.D. Pinto, W.M. Goncalves, J.C. Sartorelli, Phys. Lett. A 255 (1999) 58.

[16] K. Kiyono, N. Fuchikami, J. Phys. Society of Japan 10 (1999) 3259.

[17] A. Ilarraza-Lomelí, C.M. Arizmendi, A.L. Salas-Brito, Phys. Lett. A 259 (1999) 115.

[18] T.N. Buch, W.B. Pardo, J.A. Walkenstein, M. Monti, Epaminondas Rosa, Jr., Phys. Lett. A 248 (1998) 353.

[19] d'Innocenzo, A., Renna, L. "Dripping Faucet," Int. J. of Theor. Phys. 35(5) (1996) 941-973.